

Final Technical Report

Award Number: 03HQGR0099

Recipient: University of Texas at El Paso

Principal Investigator: Diane I. Doser

Title: **Studies of Benioff-Zone Earthquakes Within the Anchorage,
Alaska Region**

Program Element: II

Research supported by the U.S. Geological Survey (USGS), Department of the Interior, under
USGS award number 03HQGR0099

The views and conclusions contained in this document are those of the authors and should not be interpreted as necessarily representing the official policies, either expressed or implied, of the U.S. Government.

Award Number: 03HQGR0099

STUDIES OF BENIOFF-ZONE EARTHQUAKES WITHIN THE ANCHORAGE, ALASKA REGION

Diane I. Doser

The University of Texas at El Paso, Department of Geological Sciences, 500 W. University Ave., El Paso, TX 79968
(915)-747-5851 (office), (915)-747-5073 (FAX), doser@geo.utep.edu

TECHNICAL ABSTRACT:

This research focused on Benioff zone (lower plate) earthquakes of the Anchorage region (within ~150 km of Anchorage). The tasks we proposed to accomplish included: 1) detailed relocations of recent Benioff zone events (1971-present), 2) regional waveform modeling and empirical Greens function analysis of recent moderate ($M_w > 5.0$) earthquakes (1988-present) to determine focal mechanisms, seismic moments, stress drops, focal depths and fault rupture processes, 3) teleseismic and regional waveform modeling of $5.7 < m_b < 6.3$ Benioff zone earthquakes occurring up to 15 years prior to the 1964 mainshock, 4) examination of intensity data for historic and recent Benioff zone events to determine how these deeper events affect ground motion in the Anchorage region.

Our relocation results show that there are marked concentrations of seismicity at 30 to 50 km depths north of Anchorage, east of Anchorage, and in the southwestern portion of the study area. Earthquakes occurring at depths of 50 to 90 km parallel the 50 km Benioff zone contour. The increase in seismicity north of Anchorage is likely related to a tear in the downgoing plate. This seismicity extends from the lower plate into the upper plate and suggests strong coupling across the plate interface. Stress orientations of events in the upper (< 30 km) and lower (> 30 km) plate also suggest continuity in the direction of maximum compressive stress across the plate interface. This zone of concentrated seismicity is the likely nucleation zone for the 1943 $M_w=7.0$ Susitna Lowlands earthquake. A cluster of seismicity in the southwestern portion of the study area occurs near the projected edge of the subducting Yakutat block and may represent deformation of the Pacific plate beneath the edge of the Yakutat block at depths of ~60 km. An $M_w=6.8$ earthquake occurring in 1934 is likely associated with this cluster. Seismicity near Anchorage shows lineations that suggest high angle faulting within the subducting plate.

Focal mechanisms determined from first motion data for over 700 events suggest extensive compression within the downgoing plate in this region. Waveform modeling of recent (post-1980) earthquakes is currently underway to better determine fault rupture processes of events occurring near Anchorage.

We have collected intensity data for earthquakes throughout Alaska and have subdivided these data into four subregions (South-Central Alaska, Kodiak, Central Alaska, Southeast Alaska) for analysis. Events within the Prince William Sound region show similar attenuation of intensity with distance regardless of their focal depth. We are currently compiling intensity data from Canada to add to our analysis, which will be especially critical for events in the Denali and Southeast Alaska regions.

NON-TECHNICAL ABSTRACT

**STUDIES OF BENIOFF-ZONE EARTHQUAKES WITHIN THE
ANCHORAGE, ALASKA REGION**

Award Number: 03HQGR0099

Diane I. Doser

University of Texas at El Paso, Department of Geological Sciences, 500 W.
University Avenue, El Paso, TX 79968
(915)-747-5851, (915)-747-5073, doser@geo.utep.edu

NEHRP Element: II

Keywords: Seismology, source characteristics, seismotectonics

This study focuses on earthquake hazards of the Anchorage, Alaska region due to earthquakes occurring within the subducting Pacific plate. We have relocated and merged earthquake data for the 1950-2003 time period in order to examine the nature of deeper Pacific plate earthquake source zones and have modeled seismic waveforms to better understand seismic sources within the Pacific plate. We have compiled intensity information for earthquakes in the region, which provides insight into variations in ground shaking and their relationship to local geologic conditions.

Introduction:

Our research focused on Benioff zone (lower plate) earthquakes of the Anchorage region (within ~150 km of Anchorage) (Figure 1). The Anchorage area is a region of complex geology where both the Pacific plate and the Yakutat block, which is loosely coupled to the Pacific plate, are subducting beneath North America. The buoyancy of the Yakutat block causes a decrease in the angle of subduction to $\sim 3^\circ$ (Brocher et al., 1994) and strong coupling across the plate interface. The position of the Yakutat block corresponds to the largest asperity (Prince William Sound asperity) that ruptured during the 1964 great Alaska earthquake. An average of 18 m of displacement occurred along this asperity (Johnson et al., 1996).

In addition to subduction of the Yakutat block, there appears to be a tear in the subducting plate north of Anchorage (Ratchkovski and Hansen, 2002) as deduced from both an offset in seismicity observed along the Benioff zone and a rapid change in stress field within the subducting plate. Ratchkovski and Hansen (2002) suggest this tear separates the Kenai block from the McKinley block of the subducted plate.

Benioff zone earthquakes represent one of two important seismic source zones for the Anchorage region. Historically, these earthquakes have produced significant damage (intensities of VII to VIII) within the Anchorage urban region. Since these lower plate earthquakes have smaller magnitudes than events along the plate interface, they may also be expected to have shorter repeat times. The research builds upon previous teleseismic waveform modeling and relocation studies of large ($M_w > 6.0$), historic (1928-1964) earthquakes (Doser and Brown, 2002) and moderate ($M_w > 5.7$), recent, earthquakes (1964-1988) (Doser et al., 1999) in both the upper and lower plates, as well as detailed relocation studies of upper plate seismicity (1971-2001) (Flores and Doser, 2005).

Investigations Undertaken:

The tasks we proposed to accomplish in this study included: 1) detailed relocations of recent Benioff zone events (1964-present), 2) regional waveform modeling and empirical Greens function analysis of recent moderate ($M_w > 5.0$) earthquakes (1988-present) to determine focal mechanisms, seismic moments, stress drops, focal depths and fault rupture processes, 3) teleseismic and regional waveform modeling of $5.7 < m_b < 6.3$ Benioff zone earthquakes occurring up to 15 years prior to the 1964 mainshock, and 4) examination of intensity data for historic and recent Benioff zone events to determine how these deeper events affect ground motion in the Anchorage region.

Results:

Task 1 (post-1964 relocations of Benioff zone events)

Figure 2 shows ~9800 earthquakes occurring between 1964 and 2001 at depths > 30 km that have been relocated using the HypoDD technique (Waldhauser and Ellsworth, 2000) and phase data from the U.S. Geological Survey (USGS) and Alaska Earthquake Information Center (AEIC). Cross sections (location map in Figure 3) along the strike of the Benioff zone (Figure 4) and at an angle to the strike of the Benioff zone (Figures 5 through 17) illustrate the complexities of subduction within this region. The boxes surrounding the cross section lines (Figure 3) indicate which events have been projected onto which cross sections. Events of magnitude > 5.0 are indicated by stars on the cross sections. Earthquakes with $M_w > 6.5$ discussed in this report are indicated by triangles in Figure 2.

Figure 2 shows major concentrations of seismicity at depths of 30 to 50 km north of Anchorage, east of Anchorage, and in the southwestern portion of the study area. Earthquakes occurring at depths of 50 to 90 km parallel the 50 km Benioff zone contour of Plafker et al. (1994) (dashed line, Figure 2). The increase in seismicity north of Anchorage is likely related to a tear in the downgoing plate (Ratchkovski and Hansen, 2002) between the McKinley and Kenai blocks. The concentration of seismicity in the southwestern portion of the study area occurs near the projected edge of the subducting Yakutat block and may represent deformation of the Pacific plate around the edge of the Yakutat block. The seismicity east of Anchorage appears to be temporally related to the 1983 Columbia Bay earthquake sequence (with two

main events of $M_w = 6.4$ and 6.5). Note that the study area boundaries do not include the complete Benioff zone seismicity for events > 90 km depth.

Figure 4 shows seismicity parallel to the strike of the Benioff zone (N-N', Figure 3). Intense seismicity at depths of 30 to 40 km is observed at distances of 140 to 225 km along this cross section. Ratchkovski and Hansen (2002) suggest that the tear in the downgoing plate is located at ~ 220 km along this cross section. The concentration of seismicity observed at 20 to 40 km is located near the southwestern edge of the Yakutat block and may represent bending of the Pacific plate beneath the Yakutat block.

Seismicity along a cross section taken near the tear in the downgoing plate (B-B', Figure 3) shows an abrupt increase at 100 to 120 km along the cross section (Figure 6). This seismicity extends from the lower plate into the upper plate and suggests strong coupling across the plate interface. Stress orientations of events in the upper (< 30 km) and lower (> 30 km) plate also suggest continuity in the direction of maximum compressive stress (Flores and Doser, 2005) across the plate interface. This region of concentrated seismicity is the likely nucleation zone for the 1943 $M_w=7.0$ Susitna Lowlands earthquake (Flores and Doser, 2005).

Cross sections E-E' and F-F' show seismicity beneath Anchorage (Figures 9 and 10). Note the lineations in seismicity suggesting high-angle faulting in downgoing plate. These lineations are discussed in more detail below. Cross sections H-H' and I-I' (Figures 12 and 13) indicate the positions of $M_w>6.5$ earthquakes occurring in 1949 and 1954. The 1949 event occurs in a region that has been seismically quiescent since 1964. The 1954 event occurs near the point where the angle of subduction increases in a region that has been seismically active since 1964.

Cross sections of seismicity in the southwestern portion of the study area (K-K' and L-L', Figures 15 and 16) beneath Tustumena Lake indicate an unusual concentration of seismicity beneath the main Benioff zone at depths of ~ 60 km. Note that this unusual cluster is not an artifact of the selected cross section strike since it is also seen in Figure 4. An $M_w=6.8$ event in 1934 may be associated with this cluster of activity (orange star, Figure 16).

Focal mechanisms have been determined from first motion data for 713 events using the HASH algorithm of Hardebeck and Shearer (2002). Figures 18 to 21 show quality A through D events, respectively. Table 1 provides information on how focal mechanism quality is determined. Note that the focal mechanisms show predominantly reverse and reverse-oblique faulting.

Table 1 – Focal Mechanism Quality

Quality	Ave. misfit of polarities (%)	RMS fault plane uncertainty (deg)	Station distribution ratio	Percent mech. within 30° of preferred mech.
A	≤ 15	≤ 25	≥ 0.5	≥ 90
B	≤ 20	≤ 35	≥ 0.4	≥ 60
C	≤ 30	≤ 45	≥ 0.3	≥ 50
D	> 30	> 45	< 0.3	< 50

In the Tustumena Lake region A and B quality mechanisms (Figures 18 and 19) show north-south directed compression along reverse faults, consistent with the idea that these events could be related to the deformation of the Pacific plate around the edge of the Yakutat block. In contrast, the focal mechanism for the $M_w=6.8$ earthquake in 1934 (orange star, Figure 18) shows normal faulting (Doser and Brown, 2001). We plan to re-examine the waveforms for the 1934 to determine the robustness of the original modeling results, which would suggest there has been a significant change in the stress field of this region over the past 60-70 years. Several C and D quality mechanisms in the vicinity of the 1954 earthquake (orange star, figure 21) show strike-slip faulting similar to the mechanism of the 1954 event that was obtained from waveform modeling studies by Doser and Brown (2001).

Cross sections through the Anchorage region (Figures 9 and 10) suggest high angle faults dipping to either the northeast or southwest. In map view (Figure 3) the seismicity suggests north-northwest striking structures. Reverse faulting focal mechanisms in the region (Figures 19 to 21) have north-northwest striking nodal planes with nodal planes dipping at a high angle to the northeast, consistent with the seismicity patterns observed in Figures 3, 9 and 10. We are currently examining the length and width of these lineations in more detail to estimate the extent of fault systems within the slab (which will help provide maximum rupture lengths and widths for events expected on these structures). We believe the moderate magnitude (5-5.5) events occurring near Anchorage in 2002 could be related to these structures and hope to confirm this in our waveform modeling studies.

In addition to determining focal mechanisms from first motion data, we have also inverted first motion data directly to obtain stress field orientations using the method of Robinson (1999) for the regions shown by red boxes in Figure 22. The bold red lines denote the direction of maximum compressive stress (σ_1). Note that events within region 2 were subdivided by depth into 3 ranges (45-55 km, 55-65 km, > 65 km). Results from the inversion are given in Table 2.

Table 2 - Stress Orientations For Anchorage Region

Region	σ_1 (azm, plunge)	σ_3 (azm, plunge)	reference
Region 1	220, 40	100, 31	This study
Region 2 (50 km)	320,40	100,46	This study
Region 2 (60 km)	40,50	150,16	This study
Region 2 (70 km)	270,80	110,9	This study
Region 3	250,50	120,28	This study
Region 4	250,60	60,30	This study
R1	270,50	110,38	Flores and Doser (2005)
R2	260,50	110,36	Flores and Doser (2005)
R3	200,60	50,27	Flores and Doser (2005)
R4	250,50	90,38	Flores and Doser (2005)

The σ_1 orientations for regions 1, 3 and 4 are consistent with the results of Flores and Doser (2005) who analyzed events at 20 to 40 km depth in the green boxes (Figure 22), with σ_1 directions indicated by bold green lines. The direction of motion of the Pacific plate relative to North America (DeMets and Dixon, 1999) is indicated by the magenta arrow. This suggests that σ_1 throughout much of the region is not parallel to the direction of plate motion and seems to have a similar orientation from the lower crust of North America into the subducted plate, indicating strong coupling across the plate boundary. Note that there also appears to be a rotation of σ_1 near the suspected tear in the subducting plate (dashed line, Figure 22). In contrast Lu et al. (1997) determined an average direction of σ_1 based on focal mechanisms for events within the subducted plate of the entire Kenai Peninsula (top left, Figure 22) that suggested σ_1 was parallel to the strike of the Benioff zone.

The stress orientations in regions 3 and 4 near Anchorage (square) are optimum for high-angle reverse faulting striking north-northwest and dipping to the southeast, similar to the focal mechanisms determined for individual events. In region 2 the orientation of σ_1 suggests a transition from oblique-normal to high-angle normal faulting with depth. We are currently analyzing first motion data for the Tustumena Lake region to determine if it is consistent with focal mechanisms suggesting east-west oriented reverse faulting.

Task 2 (regional waveform modeling, post-1983 events)

We have collected digital waveform data for lower plate events ($M \geq 5.0$) shown in red in Figure 23 and listed in Table 3. Because many of the events within Upper Cook Inlet have similar hypocenters we are currently using the empirical Greens function technique to analyze these events.

Table 3 – Recent events for waveform modeling studies

<u>yrmoday</u>	<u>ot</u>	<u>lat</u>	<u>long</u>	<u>depth</u>	<u>mag.</u>	<u>stations</u>
19900813	2342	60.2	-151.98	87	5.3 mb	ANMO, PAS, WES
19901207	0855	61.62	-150.45	66	5 mb	ANMO, PAS, MAJO
19910426	0616	61.25	-150.15	38	5.4 mb	ANMO, COL, PAS, MAJO
19911207	1142	60.95	-150.34	50	5.2 mb	ANMO, COL, PAS, MAJO
19921202	1803	61.81	-151.19	74	5.5 mb	ANMO, COL, PAS, MAJO, WES
19920609	0720	61.33	-150.07	37	5.1 ML	ANMO, COL, PAS, MAJO
19930518	0804	61.03	-149.95	51	5.2 mb	ANMO, COL, PAS, MAJO, DUG
19940425	0019	60.9	-151.14	67	5.7 ML	ANMO, COL, KEV, PAS, MAJO
19950524	1102	61.01	-150.12	41	5.6 Mw	ANMO, COL, DUG, KEV, PAS, MAJO, WES
19960704	1139	61.85	-150.83	54	5.7 ML	ANMO, KEV, MAJO, WES
19970506	0131	61.56	-149.72	31	5.3 Mw	ANMO, DUG, KEV, MAJO
19971205	1457	60.9	-149.19	36	5.1 ML	ANMO, DUG, KEV, PAS, MAJO
199702 17	0933	61.81	-149.6	47	5 ML	ANMO, KEV, PAS, MAJO
19970513	2311	61.05	-150.77	58	5 ML	ANMO, DUG, KEV, MAJO
19980927	0057	61.57	-149.66	34	5.1 ML	ANMO, DUG, KEV, PAS, MAJO
19990722	0535	61.3	-149.38	45	5.6 ML	ANMO, DUG, KEV, PAS, MAJO, WES
19990418	1505	60.39	-151.85	73	5.3 Mw	ANMO, DUG, KEV, MAJO, PAS
19990703	1526	61.45	-150.45	60	5 mb	ANMO, DUG, KEV, PAS, MAJO
20000316	0848	61.4	-149.89	39	5.2 ML	ANMO, DUG, KEV, PAS, MAJO
20020206	1718	61.17	-149.73	35	5.3 ML	ANMO, PAS, KEV, MAJO
20020206	1719	61.18	-149.73	36	5.1 mb	ANMO, PAS, KEV, MAJO

Task 3 (teleseismic and regional waveform modeling of events occurring between 1950-1964)

We have digitized all waveforms for pre-1964 mainshock events of $M \geq 5.0$ and events occurring prior to the onset of digital recording (in ~1983) (blue diamonds, Figure 23). Table 4 summarizes data we have collected for these events. We hope to compare these to post-1964 events.

Table 4 – Pre-1964 events for waveform modeling studies

Date	lat	long	mag	stations
06/18/1934	60.217	-151.356	6.8	EDI, KEW, LPZ, PAR
10/03/1954	60.681	-150.448	6.8	ABE, DUR, EDI, HEL, KEW, LPZ, WES
06/30/1960	60.41	-150.77	5.9	WES

Task 4 (analysis of intensity information)

We have collected intensity data for earthquakes occurring throughout Alaska and have divided the earthquakes into 4 regions (South-Central Alaska, Kodiak, Central Alaska, Southeastern Alaska) for further analysis. Our primary sources of data are from the NOAA intensity web site (http://www.ngdc.noaa.gov/seg/hazard/int_srch.shtml) for events occurring between 1964 and 1985. In addition, we have used zip code/internet response-based intensity information collected from the USGS’s “Did You Feel It?” data archive (pasdena.wr.usgs.gov/shake/ak) for events occurring since 1999 and are currently obtaining intensity data for Canada from colleagues at the Pacific Geoscience Centre. Intensity versus median distance for calibration events within these 4 regions are shown in Figures 24 and 25. Calibration events were required to have observations of intensity from at least 17 different localities and to have observations of at least 3 different intensity levels. We will use these calibration events to

develop intensity/distance attenuation relationships and then test the ability of these relationships to help locate and estimate magnitudes for a set of test events (generally of smaller magnitude with less intensity observations) that have occurred since 1964. Finally, we will use our refined relationships to better determine the locations and magnitudes of pre-1964 events.

For the South-Central Alaska region (Figure 24) the pattern of the fall-off of intensity with distance is very similar for the 1964 great Alaska mainshock, lower plate events in 1968, 1982 and July 1983 (Columbia Bay), and the 1984 crustal Sutton earthquake. All events have $M_w \geq 5.7$. The February 2002 event occurred nearly directly beneath Anchorage so that intensity variations appear to have been strongly controlled by near site effects, since many sites were nearly equidistant from the earthquakes. The September 1983 Columbia Bay event ($M_w=6.4$) exhibits a different fall-off in intensity than the July 1983 event. The September event occurred very close to the hypocenter of the July 1983 event, but had a slightly different focal mechanism. These preliminary results suggest that events of $M_w \geq 5.7$, regardless of position (crust, interface, subducted slab), may create similar amounts of shaking. This could make it difficult to use intensity information from historical events to help estimate event focal depth. The 2002 events may also serve as a good model for intensity fall-off for larger events occurring directly beneath Anchorage.

Intensity results for the Kodiak region (Figure 24) show the effects of sparser population within the epicentral region, possible depth effects (most events shown had focal depths > 60 km) and possible wave propagation effects. It appears that the subducted slab acts as a wave guide that creates stronger shaking along the strike of the subduction zone that perpendicular to it.

Data from Canada are needed to provide better azimuthal and distance coverage for Southeastern Alaska and for a number of Denali fault events (Figure 25). The 2002 Denali fault mainshock is also likely to be influenced by rupture directivity. Once we are confident that all possible data have been collected for these regions we hope to compare how attenuation may differ between regions.

Related Studies

In addition to progress toward our four tasks outlined above, we have conducted studies of crustal seismic moment rates in the Anchorage region. Our seismic moment rate calculations show a factor of 1000 decrease in moment rates following the 1964 mainshock. We then used geologic information on structures within Cook Inlet basin (e.g. Haeussler et al., 2000) to estimate a regional geologic moment rate. Since it is difficult to estimate the amount of horizontal offset that has occurred along these structures, our geologic moment rates could underestimate the true rates by up to 70%. Nevertheless, the geologic moment rate is only 4 to 10 times lower than the pre-1964 mainshock seismic moment rate. This suggests that the 1964 mainshock has significantly slowed regional crustal deformation. If we compare the geologic moment rate to the post-1964 mainshock rate, the moment rate deficit over the past 36 years is equivalent to an M_w 6.5 to 6.8 earthquake. This highlights the difficulty in using seismicity in the decades following a large megathrust earthquake to adequately characterize long-term crustal deformation. These results were published in the *Bulletin of the Seismological Society of America* (Doser et al., 2004).

We have also studied seismic moment rates for crustal, interface and intraslab regions of the Prince William Sound (PWS) and Kodiak asperities using data for $M > 5.5$ earthquakes occurring over the past 70+ years. It appears there has been a decrease in seismic moment release (factor of 5 to 10) in both the crust and slab of the PWS asperity region since 1964. In contrast moment release in the Kodiak asperity region has increased by a factor of 2. We plan to submit the results of this study to a professional journal by the end of 2005.

A paper on historical seismicity of the Denali fault zone was published in a special issue of the *Bulletin of the Seismological Society of America* (Doser, 2004). The paper concentrated on seismicity prior to 1971, although earthquakes occurring between 1971 and 1998 were relocated. In addition to the relocations, waveform modeling for events of $M > 6.0$ were conducted. The waveform modeling and earthquake locations suggest that most $M > 6.0$ events occurred on strike-slip or reverse faults located either south or north of the Denali fault. A magnitude 6.5 event in 1929 appears to have occurred within

the subducting slab at a depth of ~ 60 km. Events in 1962 appear to have occurred upon a reverse fault that may be the extension of the Pass Creek fault. A magnitude 6.9 event in 1932 appears to be a deeper event (~30-40 km) along a left-lateral strike-slip fault. Of considerable interest is the July 7, 1912 earthquake (M~7.2). This has been relocated to the vicinity of the Denali fault, although its 95% confidence ellipse is very large. Surface wave and body wave amplitudes observed for two stations (Riverview, Australia and Honolulu, Hawaii) are not inconsistent with rupture along the Denali fault. If the 1912 event actually occurred on the Denali fault, this may explain why the portion of the Denali fault located between the October 2002 Nenana Mountain rupture zone and the November 2002 Denali rupture zone was relatively aseismic during the 2002 sequence.

A paper on the crustal seismicity (< 40 km depth) of the Anchorage study area is in press in the *Bulletin of the Seismological Society of America* (Flores and Doser, 2005). We have relocated over 4200 shallow (≤ 40 km) earthquakes occurring in the Anchorage region for ~35 years following the 1964 great Alaska earthquake. The shallowest (< 20 km) earthquakes delineate several faults within the crust, including one associated with mapped folds located north of Upper Cook Inlet. Inversion of first motion data for the stress field orientation in Upper Cook Inlet indicates east-west oriented horizontal σ_1 and near vertical σ_3 , a condition favoring reverse faulting along east-west striking faults with trends similar to the orientation of mapped faults and fault cored anticlines within the inlet. σ_1 is rotated 60° to 90° counterclockwise from the direction of plate convergence, in agreement with GPS/geodesy studies that indicate the western portion of the Kenai Peninsula and upper Cook Inlet do not appear to be moving in the direction plate motion due to a change in coupling across the plate interface. The stress regime north of the Castle Mountain fault is conducive to strike-slip or normal faulting along faults striking east-northeast or north-northwest. Similar to previous studies we observed a persistent zone of seismic quiescence in the upper crust that appears to be located above and immediately downdip of the portion of the plate interface that slipped 20-25 m in the 1964 mainshock. Deeper (20 to 40 km) earthquakes indicate intense deformation and a rapidly changing stress field near the boundary between the Kenai and McKinley segments of the subducted slab. The 1943 $M_w=7.0$ Susitna lowlands earthquake may have been associated with this region of complex deformation.

A paper on the historical seismicity of the Kodiak Island region was published in the *Bulletin of the Seismological Society of America* (Doser, 2005). Thirty-five earthquakes were relocated and waveform modeling studies of 12 events were conducted. The events were located primarily within the Kodiak portion of the 1964 great Alaska earthquake rupture zone and the northeasternmost portion of the 1938 Semidi earthquake rupture zone. These results show that there is considerable similarity between pre-1964 mainshock seismicity and post-1964 mainshock seismicity. Persistent seismicity has occurred for the past ~85 years at the southwestern end of the 1964 rupture zone, a region where GPS/geodesy studies indicate the plate interface is currently locked. Earthquakes also occurred frequently within the Kennedy Entrance region where the transition between the Kodiak and Kenai block of the subducting Pacific plate occurs.

Finally, we have collected waveform and phase data for the southern Kenai Peninsula/Prince William Sound region for analysis similar to that we have conducted for the Anchorage region for use in a funded NEHRP project that began June 1, 2005.

Reports Published:

Doser, D.I., N. Ratchkovski, P. Haeussler, and R. Saltus, Changes in crustal seismic deformation rates associated with the 1964 great Alaska earthquake, *Bull. Seismol. Soc. Amer.* **94**, 320-325, 2004.

Doser, D.I., Seismicity of the Denali-Totschunda Fault Zone in Central Alaska (1912-1988) and its Relation to the 2002 Denali Fault Earthquake Sequence, *Bull. Seismol. Soc. Amer.* **94**, S132-144, 2004.

Doser, D.I., Historical Seismicity (1918-1964) of the Kodiak Island Region, *Bull. Seismol. Soc. Amer.* **95**, 878-895, 2005.

Flores, C., and D.I. Doser, Shallow Seismicity of the Anchorage, Alaska Region (1964-1999), in press, October issue, *Bull. Seismol. Soc. Amer.*, 2005.

Availability of Data Sets:

Copies of phase data, intensity data, first motion data, and waveform data are also available in digital form. Contact the principal investigator, Dr. Diane Doser, for more details at (915)-747-5851 or doser@geo.utep.edu.

Bibliography

Brocher, T.M., G.S. Fuis, M.A. Fisher, G. Plafker, M.J. Moses, J.J. Taber, and N.I. Christensen (1994). Mapping the megathrust beneath the northern Gulf of Alaska using wide-angle seismic data, *J. Geophys. Res.* **99**, 11,663-11,686.

DeMets, C., and T.H. Dixon (1999). New kinematic models for Pacific-North America motions from 3 Ma to present, 1: Evidence for steady motion and biases in the NUVEL-1A model, *Geophys. Res. Lett.* **26**, 1921-1924.

Doser, D.I., and W.A. Brown (2001). A study of historic earthquakes of the Prince William Sound, Alaska region, *Bull. Seism. Soc. Am.* **91**, 842-857.

Doser, D.I., A. Veilleux, and M. Velasquez (1999). Seismicity of the Prince William Sound Region for Thirty Two Years Following the 1964 Great Alaskan Earthquake, *Pure and Appl. Geophys.* **154**, 593-632.

Haeussler, P.J., R. L. Bruhn, and T.L. Pratt (2000). Potential seismic hazards and tectonics of Upper Cook Inlet Basin, Alaska, based on Pliocene and younger deformation, *Geol. Soc. Am. Bull.* **112**, 1414-1429.

Hardebeck, J.L., and P. M. Shearer (2002). A new method for determining first-motion focal mechanisms, *Bull. Seismol. Soc. Am.* **92**, 2264-2276.

Johnson, J.M., K. Satake, S.R. Holdahl, and J. Sauber (1996). The 1964 Prince William Sound earthquake: Joint inversion of tsunami and geodetic data, *J. Geophys. Res.* **101**, 523-532.

Lu, Z., M. Wyss, and H. Pulpan (1997). Details of stress directions in the Alaska subduction zone from fault plane solutions, *J. Geophys. Res.* **102**, 5385-5402.

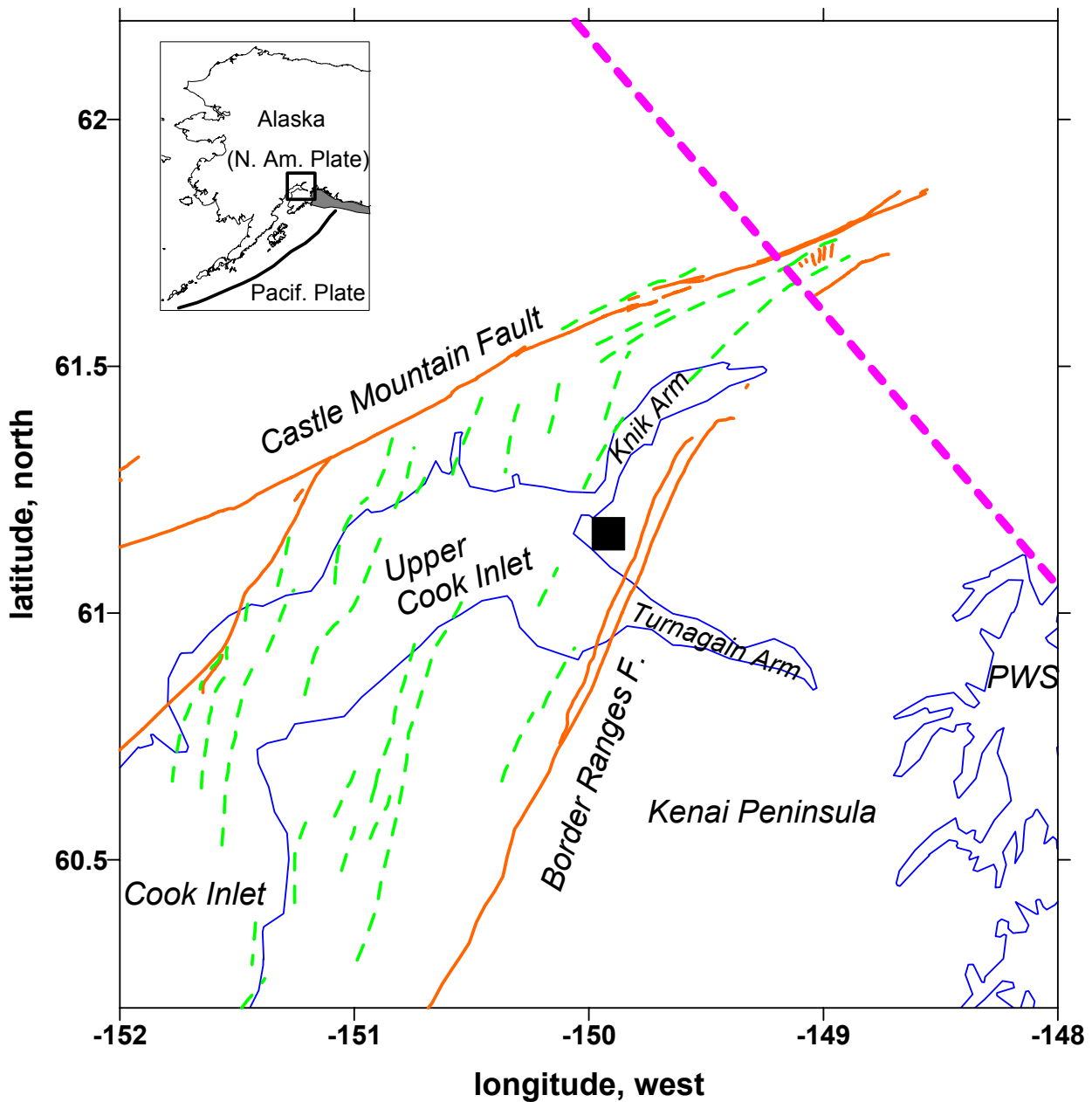
Plafker, G., L.M. Gilpin, and J. C. Lahr (1994). Neotectonic map of Alaska, in *The Geology of North America*, vol. **G-1**, The geology of Alaska (G. Plafker and H.C. Berg, eds.), Geol. Soc. Amer., Boulder, Colo., pp. 389-449.

Ratchkovski, N.A., and R.A. Hansen (2002). New evidence for segmentation of the Alaska subduction zone, *Bull. Seismol. Soc. Am.* **92**, 1754-1765.

Robinson, R. (1999). Get Stress: A Computer Programme for Inverting First Motion Observations to a Regional Stress Tensor, Institute of Geological and Nuclear Sciences, Lower Hutt, New Zealand, 7 pp. (copy of software available at ftp.gns.cri.nz/pub/robinson/getstress).

Waldhauser, F., and W.L. Ellsworth (2000). A Double-Difference earthquake location algorithm: method and application to the northern Hayward fault, California, *Bull. Seismol. Soc. Am.* **90**, 1353-1368.

Figure 1 - Anchorage study area. Inset map shows location of study area with respect to the North American and Pacific plates. Solid line on inset map is Aleutian trench, grey area is Yakutat block. Square denotes Anchorage. Green dashed lines are Neogene folds and orange solid lines are Neogene faults from Haeussler et al. (2000). Magenta dashed line is the tear in the subducting plate as located by Ratchkovski and Hansen (2002). PWS is Prince William Sound.



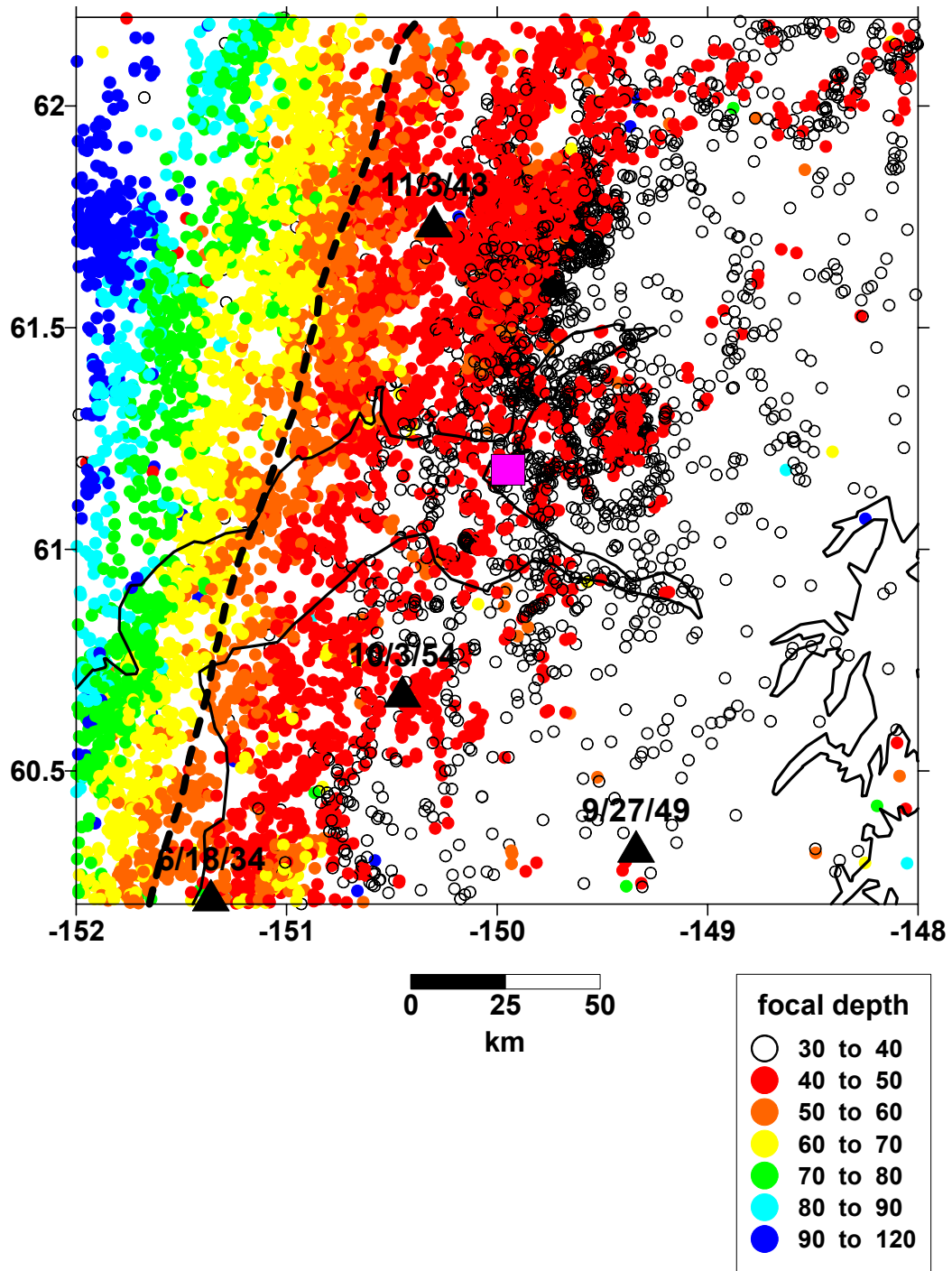


Figure 2 - Relocated earthquakes occurring between 3/29/1964 and 12/31/2001 with depths > 30 km. Dashed line represents 50 km. Wadati-Benioff zone contour is from Plafker et al. (1994). Triangles are events with moment-magnitude > 6.5 and focal depths > 25 km. Square denotes Anchorage.

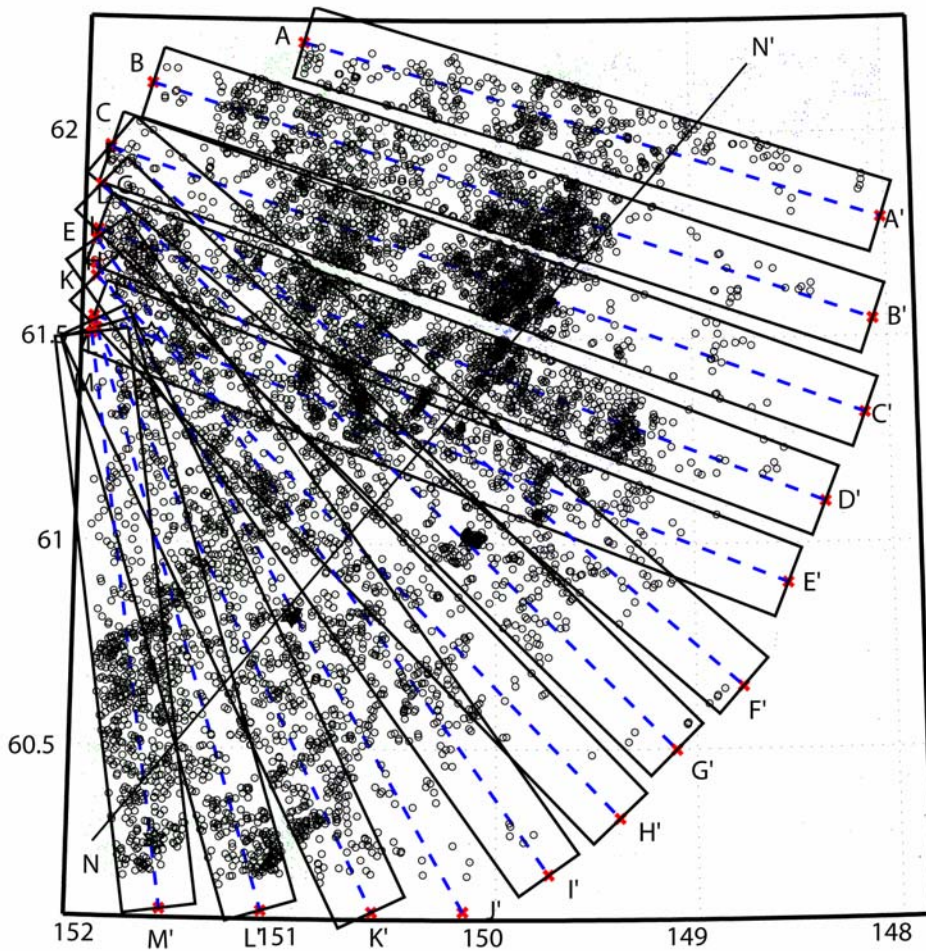


Figure 3 – Map of seismicity indicating location of cross sections A-A' through N-N' shown in Figures 4 through 17.

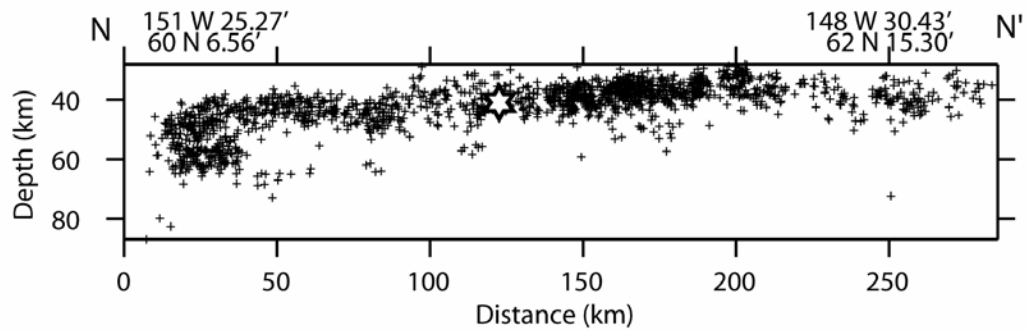


Figure 4 – Cross section along strike of Benioff zone. See Figure 3 for cross section location. Stars denote magnitude ≥ 5.0 events.

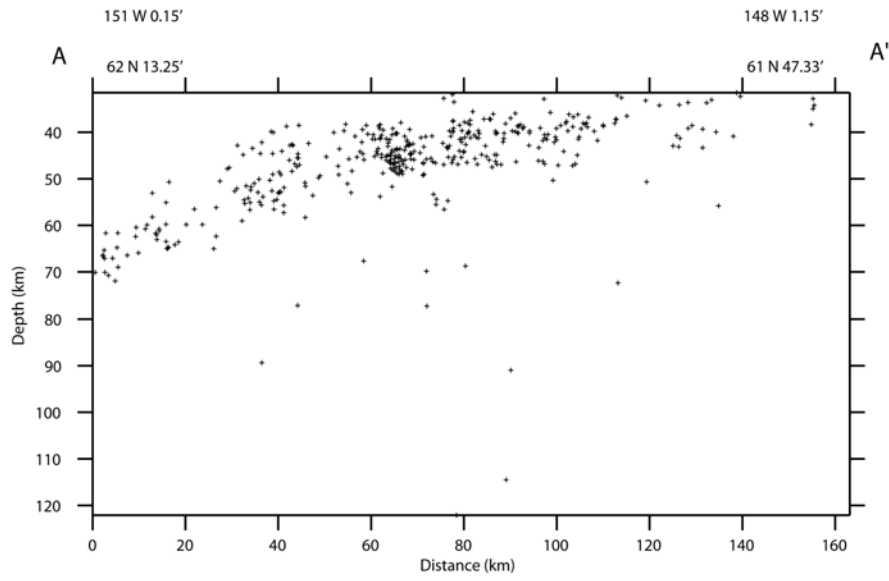


Figure 5 – Cross section along A-A'. See Figure 3 for cross section location.

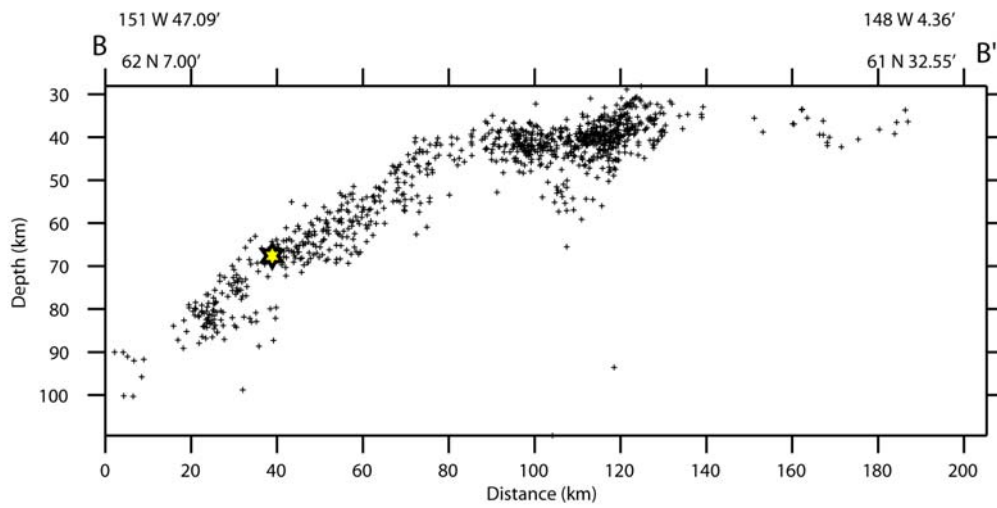


Figure 6 – Cross section along B-B'. See Figure 3 for cross section location.

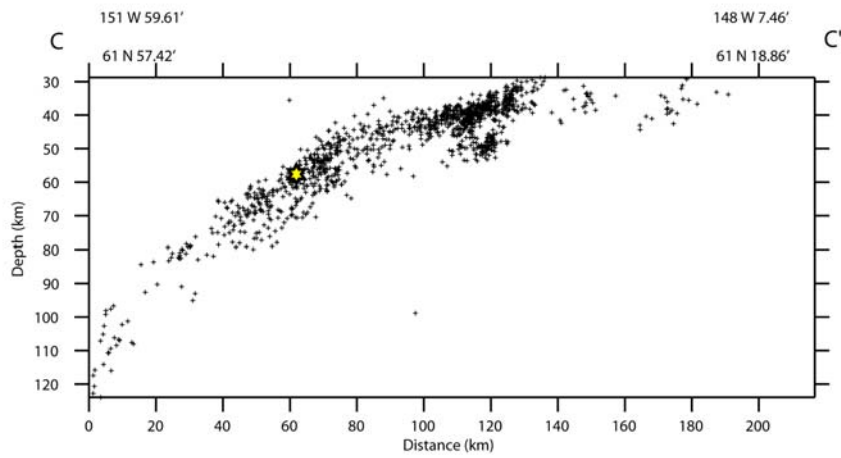


Figure 7 – Cross section along C-C'. See Figure 3 for cross section location.

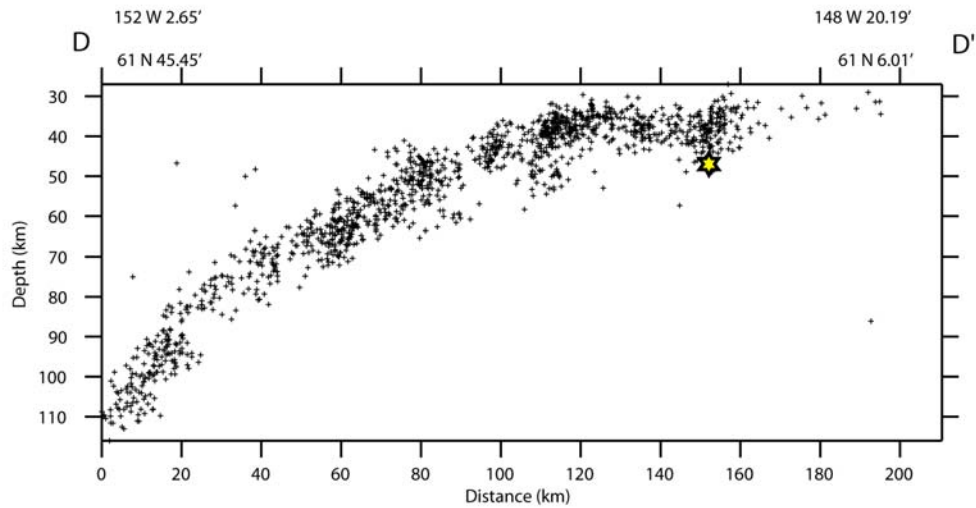


Figure 8 – Cross section along D-D'. See Figure 3 for cross section location

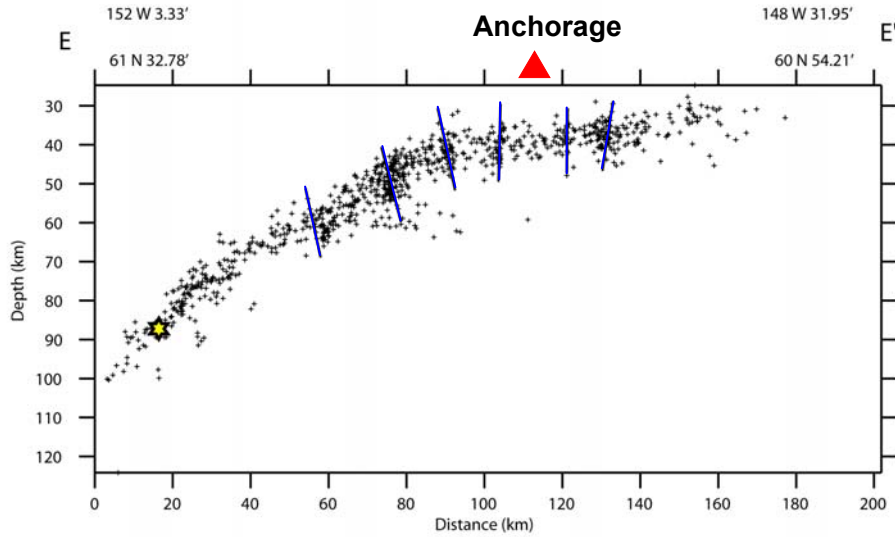


Figure 9 – Cross section along E-E'. Triangle denotes position of Anchorage. See Figure 3 for cross section location. Blue lines indicate possible lineations in seismicity.

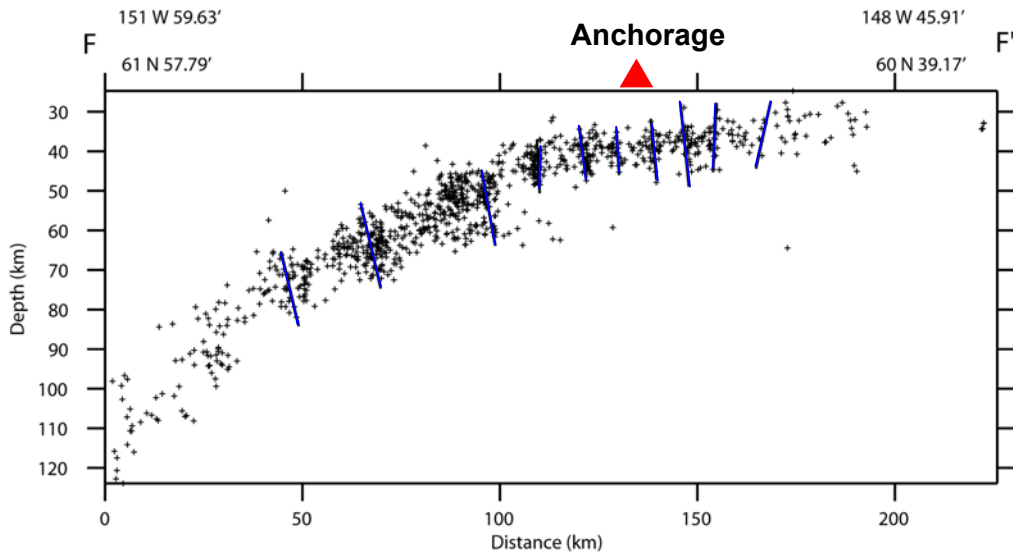


Figure 10 - Cross section along F-F'. Triangle denotes position of Anchorage. See Figure 3 for cross section location. Blue lines indicate possible lineations in seismicity.

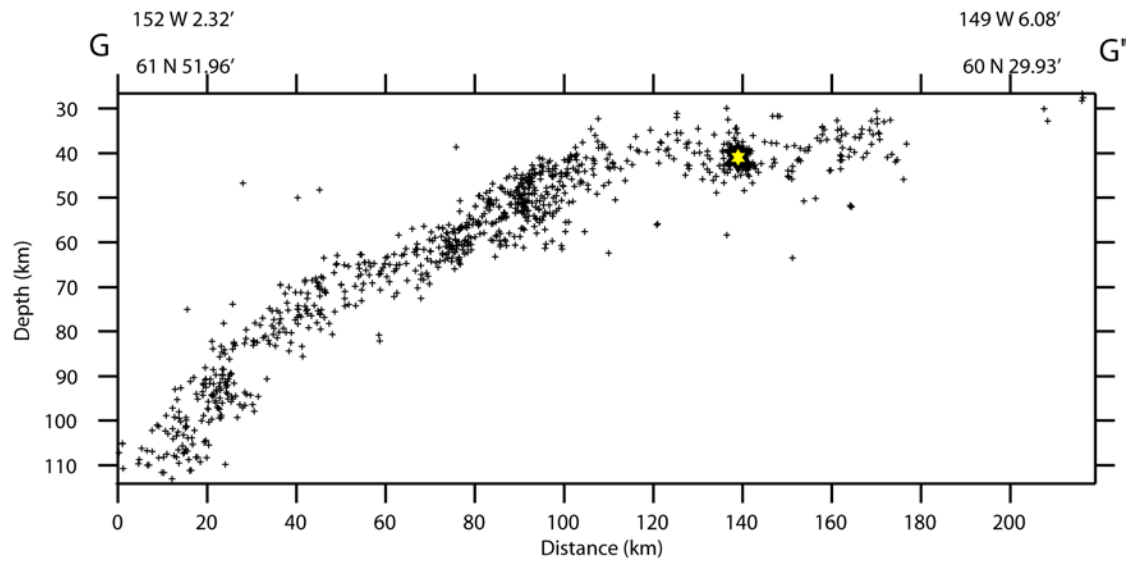


Figure 11 – Cross section along G-G'. See Figure 3 for cross section location.

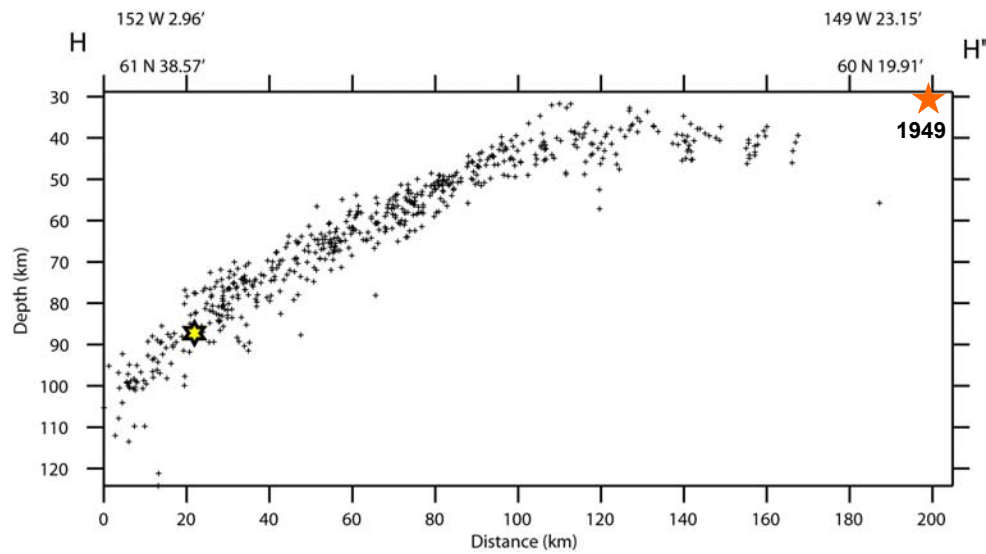


Figure 12 – Cross section along H-H'. See Figure 3 for cross section location. Orange star is the location of a moment-magnitude 6.7 earthquake that occurred in 1949.

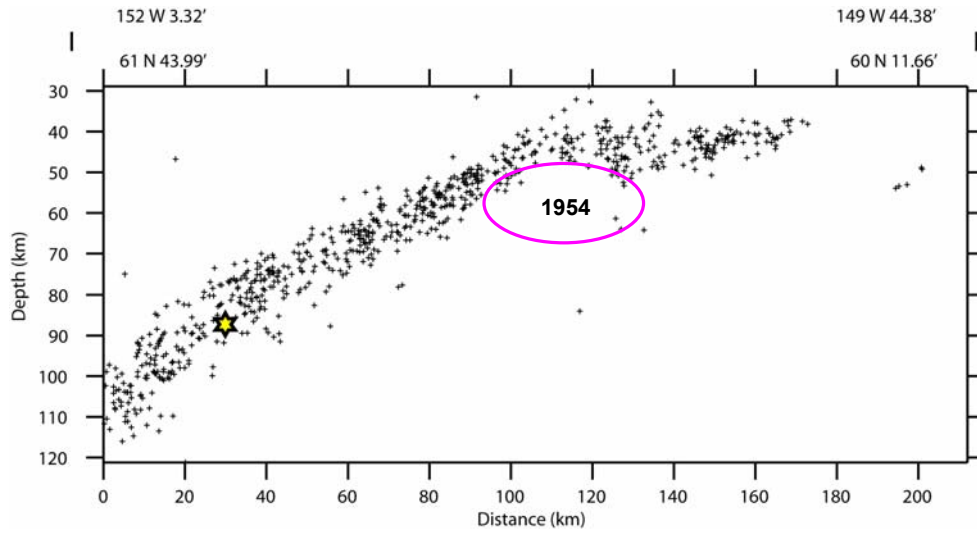


Figure 13 – Cross section along I-I'. See Figure 3 for cross section location. Ellipse is 95% confidence ellipse for a moment-magnitude 6.8 earthquake that occurred in 1954.

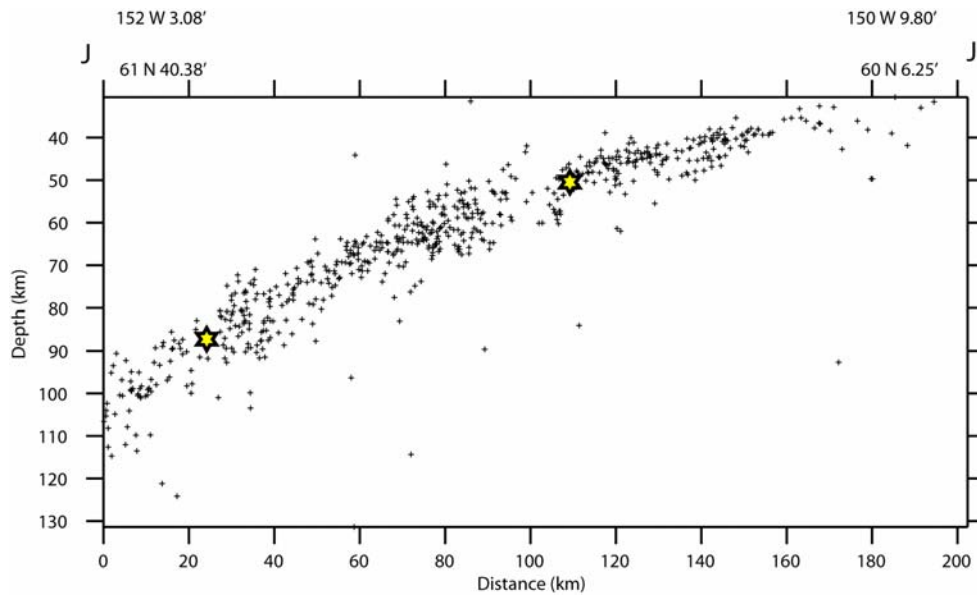


Figure 14 – Cross section along J-J'. See Figure 3 for cross section location.

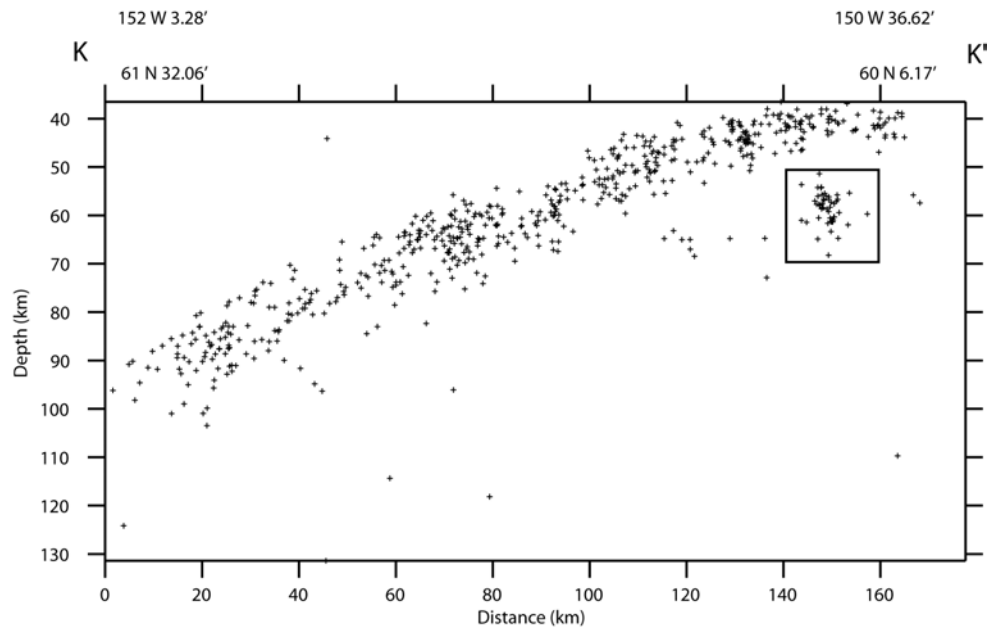


Figure 15 – Cross section along K-K'. See Figure 3 for cross section location. Box indicates cluster of seismicity that may be related to deformation at the edge of the Yakutat block.

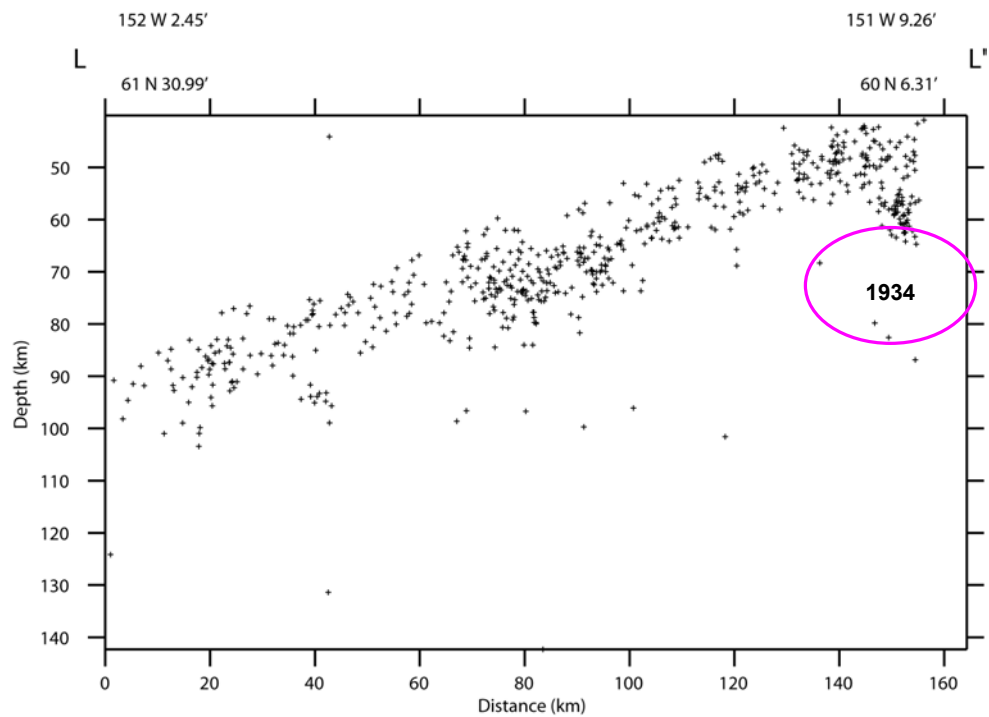


Figure 16 – Cross section along L-L'. See Figure 3 for cross section location. Ellipse is 95% confidence ellipse for location of a 1934 earthquake of moment-magnitude 6.8.

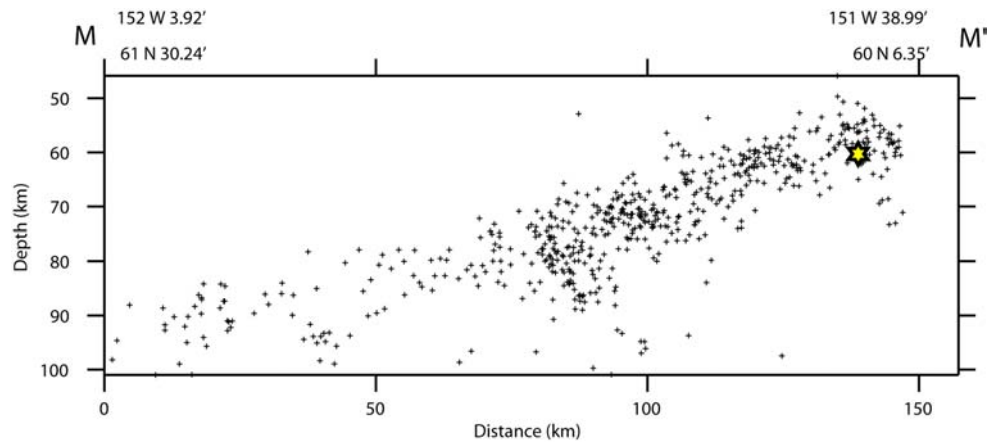


Figure 17 – Cross section along M-M'. See Figure 3 for cross section location.

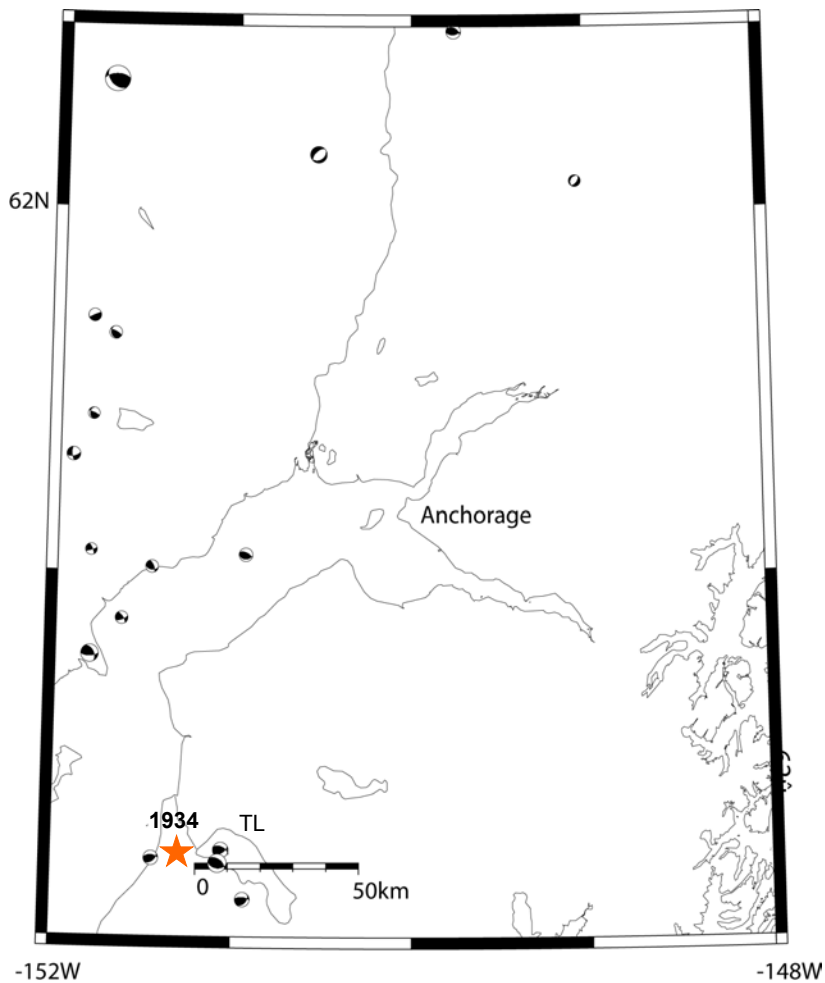


Figure 18 – A-quality focal mechanisms from HASH (Hardebeck and Shearer, 2002) routine. Star is location of moment-magnitude 6.8 earthquake. TL indicates Tustumena Lake.

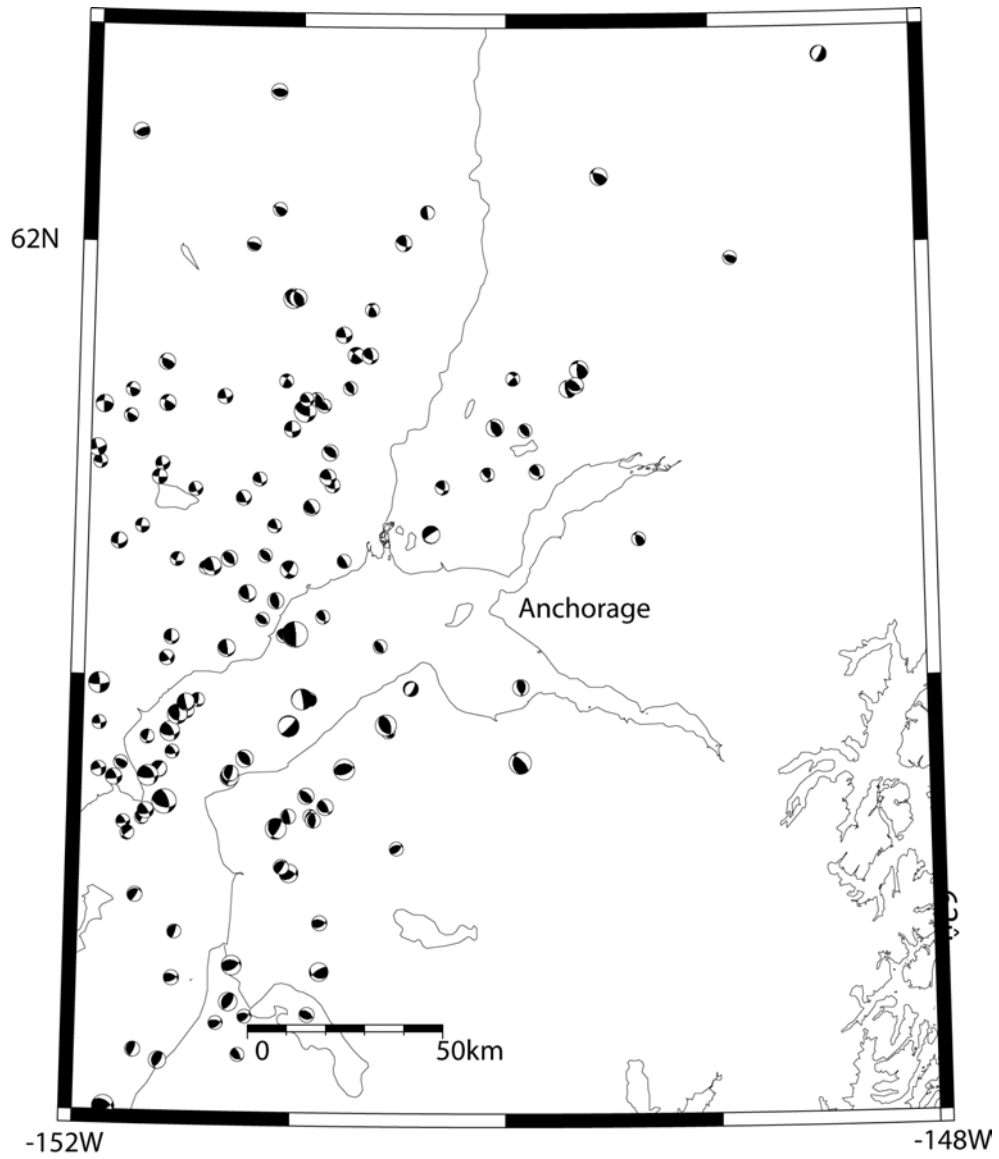


Figure 19 – B-quality focal mechanisms from HASH (Hardebeck and Shearer, 2002) routine.

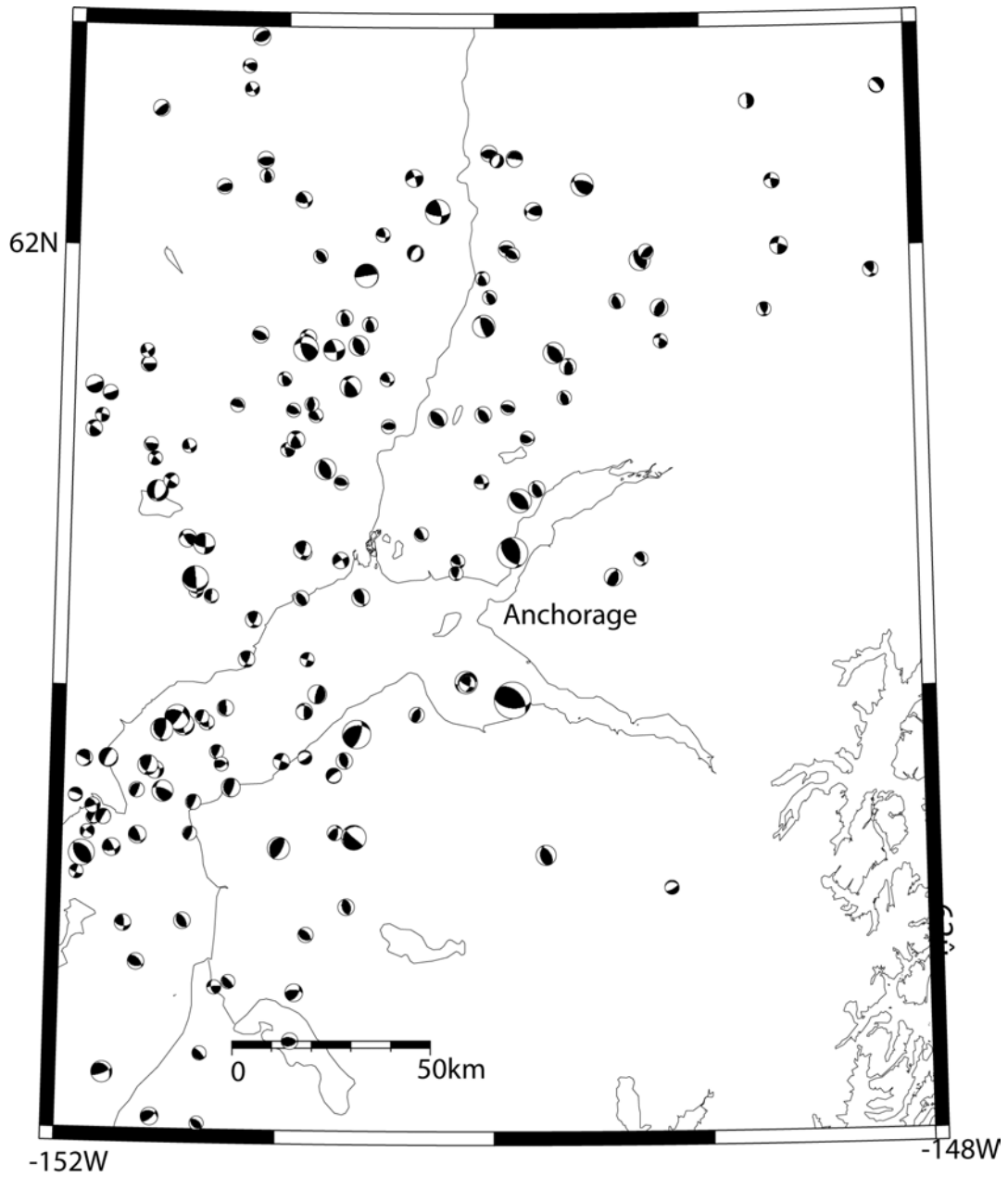


Figure 20 – C-quality focal mechanisms.

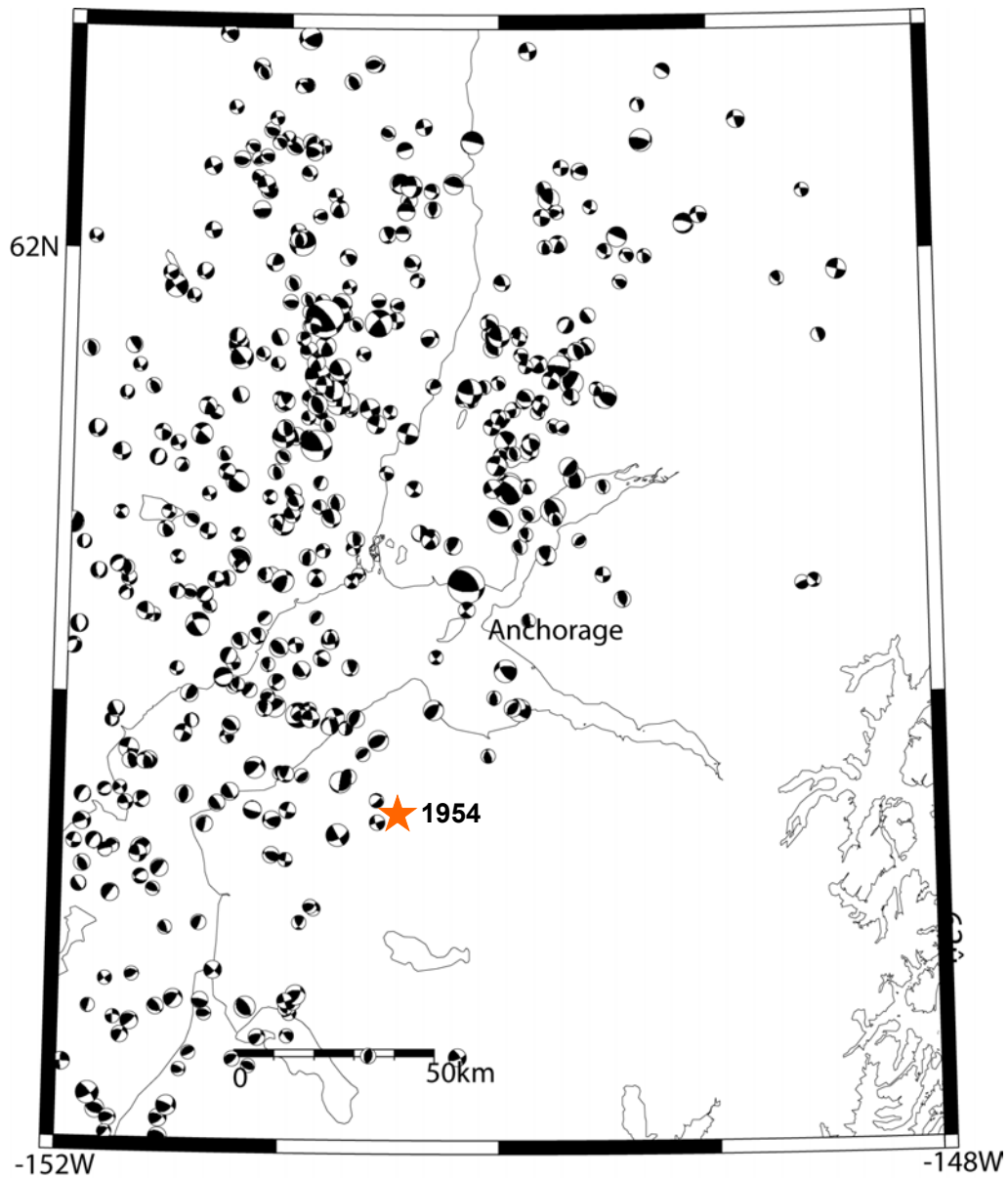


Figure 21 – D quality focal mechanisms. Star is location of moment-magnitude 6.8 earthquake in 1954.

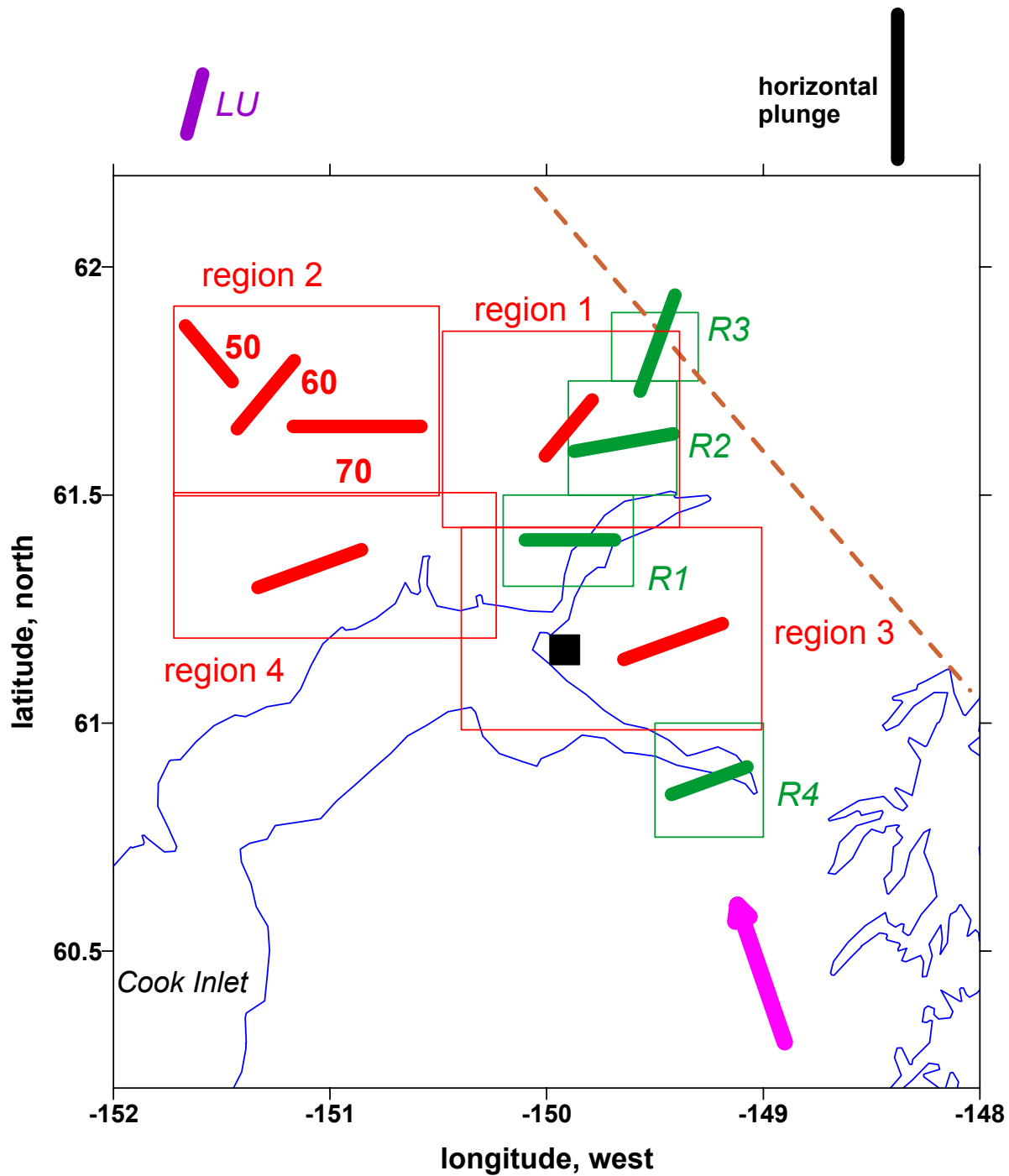


Figure 22 - Orientation of maximum compressive stress for the Anchorage region. Lengths of lines are proportional to axes plunge with horizontal plunge length indicated at top right. Boxes indicate regions where stress inversions were performed. Red boxes and lines are from this study. Green boxes and lines are from Flores and Doser (2005). Arrow is direction of motion of the Pacific plate relative to North America from DeMets and Dixon (1999). For region 2 stress orientations were estimated at 50, 60 and 70 km depth as indicated. Purple line is maximum compressive stress orientation from Lu et al. (1997). Dashed line indicates location of tear in the subducting plate from Ratchkovski and Hansen (2002).

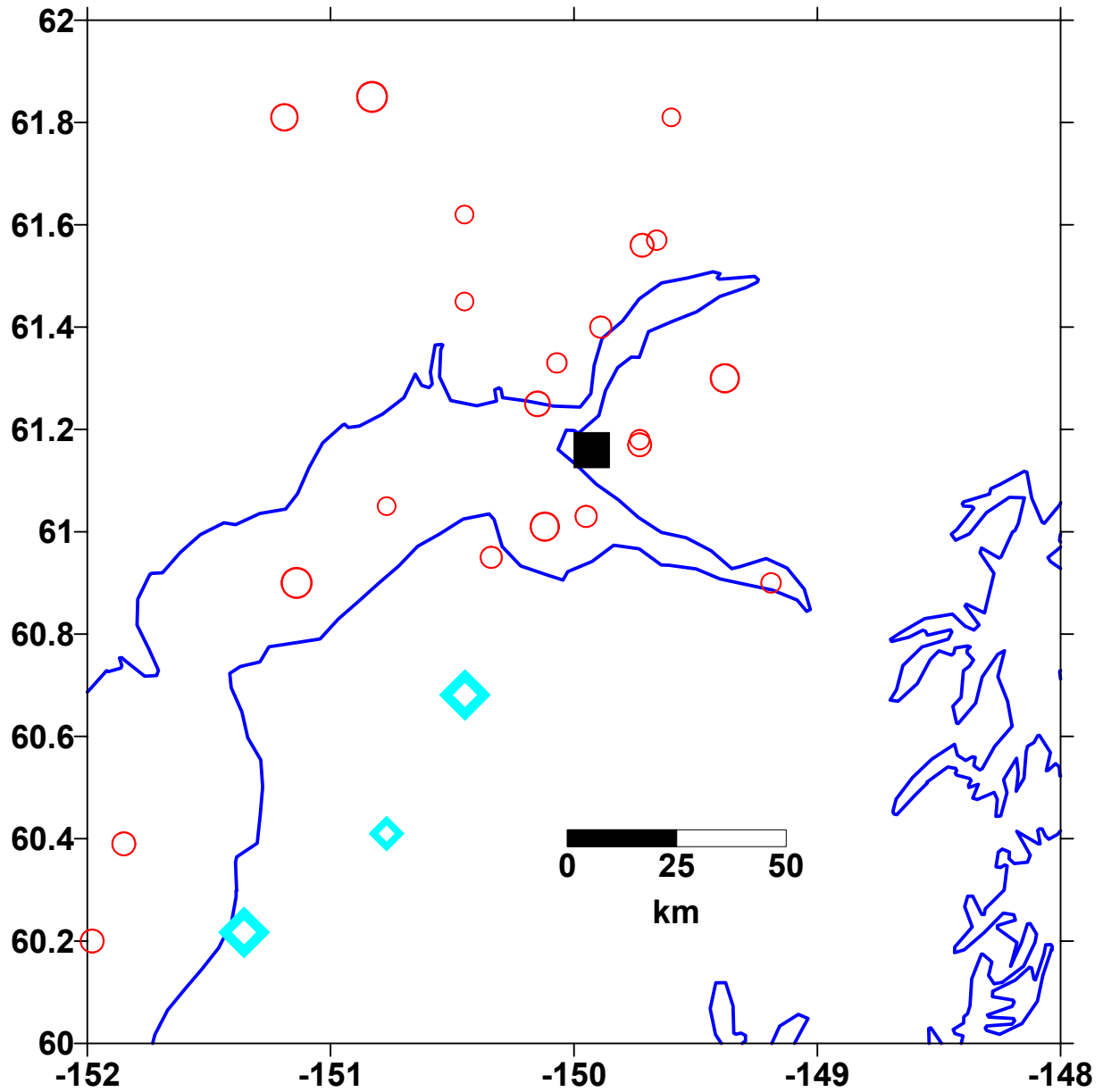


Figure 23 - Map of Anchorage study area with locations of post-1964 earthquakes (circles) and pre-1964 mainshock earthquakes (diamonds) for waveform modeling studies. Symbol size is proportional to magnitude. Square is Anchorage.

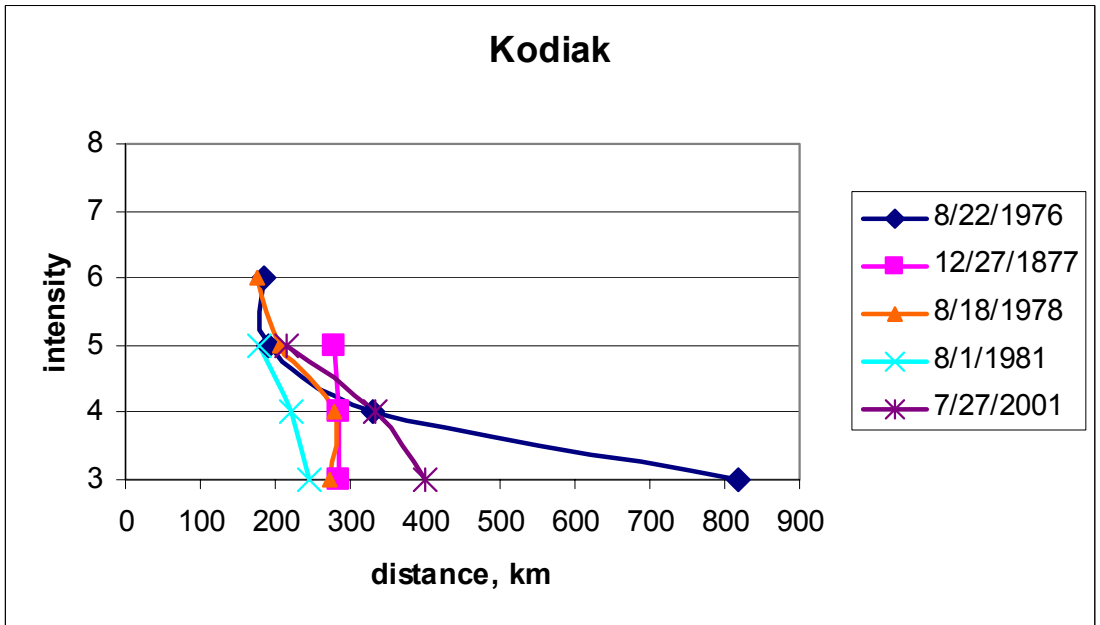
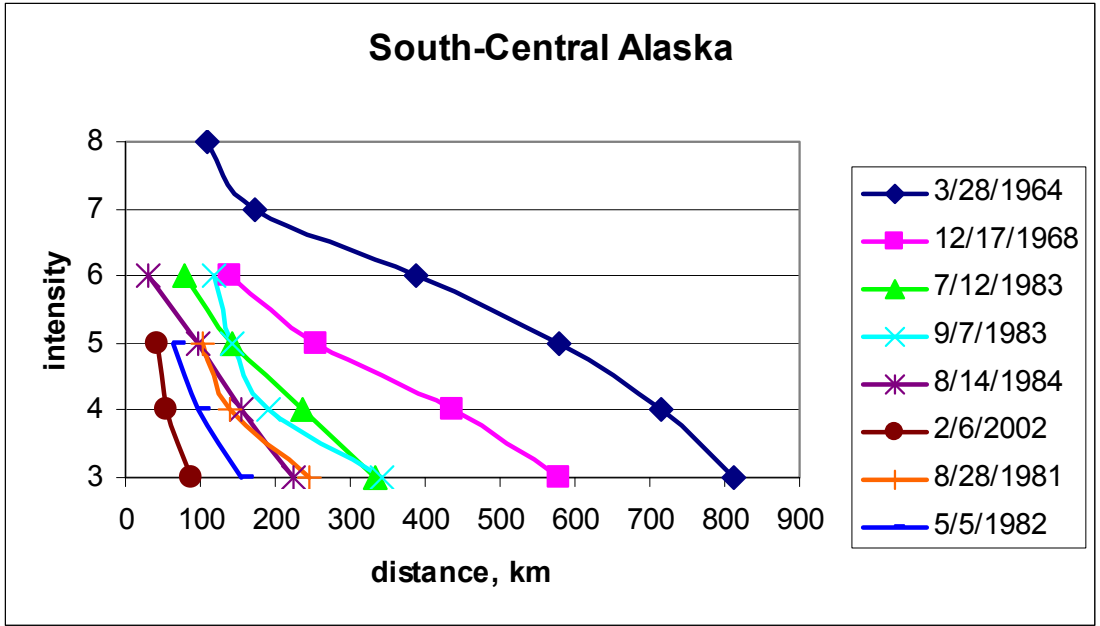


Figure 24 - Median intensity versus distance for calibration events in the South-Central (top) and Kodiak (bottom) regions.

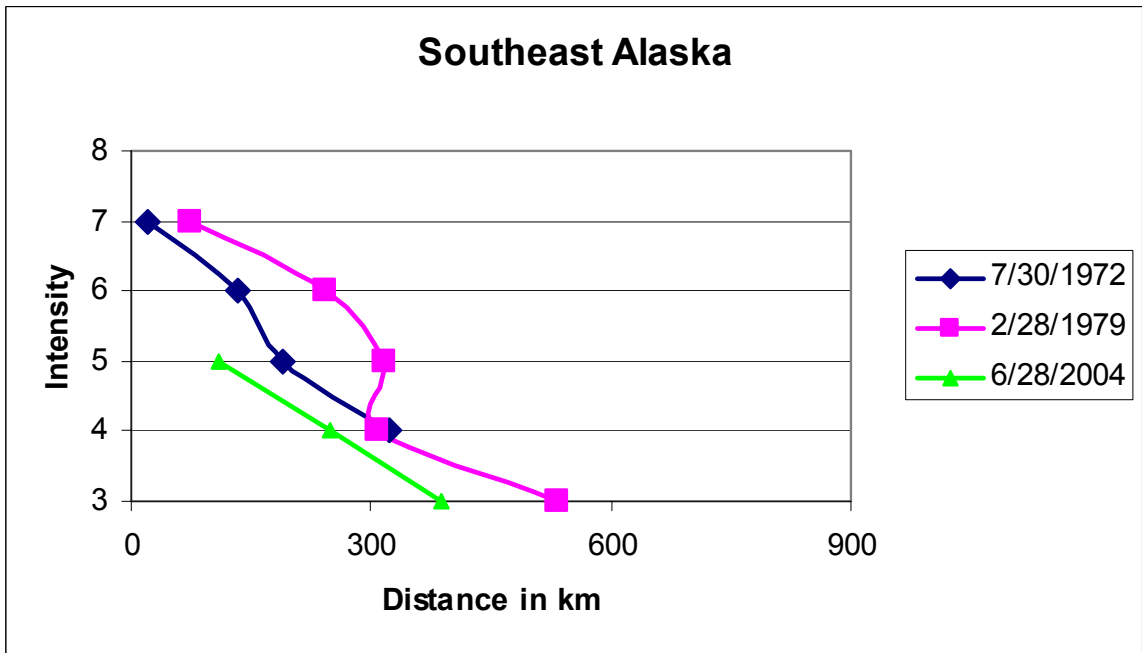
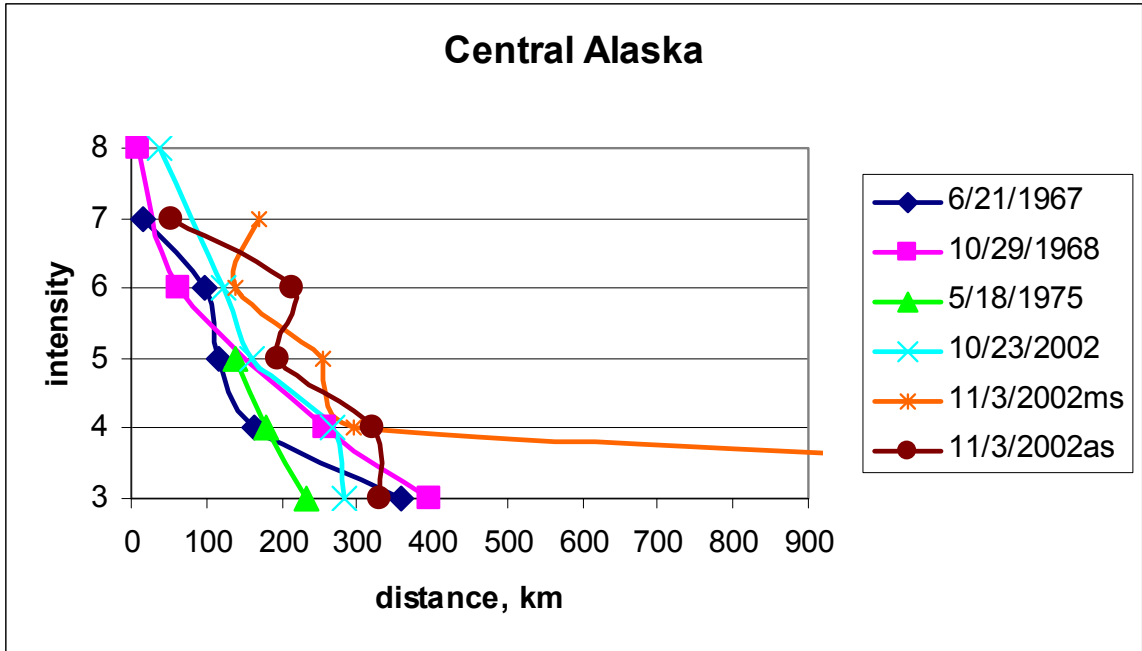


Figure 25 - Median intensity versus distance for events in the Central Alaska (top) and Southeast Alaska (bottom) regions. ms is Denali fault mainshock and as is Denali fault aftershock.